Light-sheet optimization for microscopy

Wilding, Dean; Pozzi, Paolo; Soloviev, Oleg; Vdovine, Gleb; Verhaegen, Michel

DOI
10.1117/12.2210912

Publication date
2016

Document Version
Final published version

Published in
Proceeedings of SPIE

Light-sheet optimization for microscopy

Dean Wilding[a], Paolo Pozzi[a], Oleg Soloviev[a,b], Gleb Vdovin[a,b], and Michel Verhaegen[a]

[a]Delft Center for Systems and Control, Delft University of Technology, Mekelweg 2, 2628 CD Delft, the Netherlands
[b]Flexible Optical B.V., Polakweg 10-11, 2288 GG Rijswijk, the Netherlands

ABSTRACT

Aberrations, scattering and absorption degrade the performance light-sheet fluorescence microscopes (LSFM). An adaptive optics system to correct for these artefacts and to optimize the light-sheet illumination is presented. This system allows a higher axial resolution to be recovered over the field-of-view of the detection objective. It is standard selective plane illumination microscope (SPIM) configuration modified with the addition of a spatial light modulator (SLM) and a third objective for the detection of transmitted light. Optimization protocols use this transmission light allowing the extension the depth-of-field and correction of aberrations whilst retaining a thin optical section.

Keywords: Adaptive optics, imaging, microscopy, light-sheet microscopy, optimization

1. INTRODUCTION

The light-sheet fluorescence microscope[1,2] (LSFM) is gaining increasing reputation as a tool for biomedical research.[3] The practical advantages of this microscope come from the combination of wide-field imaging speed with the optical sectioning ability of the confocal microscope.

The LS microscope is a trade off between the two methods and it works by delivering its illumination orthogonal to the fluorescence detection axis, therefore, only the imaged plane is illuminated, see Figure 1 for the layout of the microscope. This property of the illumination allows the microscope to have lower photo-bleaching and toxicity when imaging samples than the confocal microscope.[3] This makes the LSFM a highly efficient imaging technique with great future potential for biomedical research.

LSFM is similar to the confocal microscope in the sense that the point-spread function (PSF) of the microscope is the product of the illumination profile and the detection PSF, therefore, to have the best axial resolution a thin light-sheet is required. A thin light-sheet is best generated using a high NA objective with cylindrical optics to limit the illumination of the back aperture in one direction; however, with the working distance of modern objective lens being much smaller than their physical size, a compromise to the NA must be made in order to place two of them orthogonally.

This spatial hindrance of placing two high numerical aperture (NA) objective lens orthogonally is a major drawback with LSFM. It imposes difficulties not only in limiting the resolution, but also in the preparation and mounting of samples and in the delivery of the illumination. In general, samples in LSFM are mounted and prepared in a different way to the vast majority of microscopy techniques; using a capillary and embedding the samples in a stiff agarose gel. There have been attempts to return to standard preparation and mounting techniques by changing the method of light delivery, each of these techniques have their own advantages and disadvantages.[4,5]

Furthermore, when using a high NA objective lens to focus a laser beam the Gaussian beam waist, w_0, is only quasi-uniform over a small range known as the Rayleigh range, z_R.[6] Hence, for a high resolution in three dimensions it is required to use a small field-of-view (FOV), hereby limiting the applicability of this technique for some applications. The axial resolution, the optical sectioning, and the image contrast are non-uniform over the FOV. In summary, the image quality at the edges of the FOV are worse than at the center.

Further author information: (Send correspondence to D.W.)
D.W.: E-mail: d.wilding@tudelft.nl, Telephone: +31 15 278 1758

Adaptive Optics and Wavefront Control for Biological Systems II, edited by Thomas G. Bifano, Joel Kubby, Sylvain Gigan,
Proc. of SPIE Vol. 9717, 971718 · © 2016 SPIE · CCC code: 1605-7422/16/$18 · doi: 10.1117/12.2210912

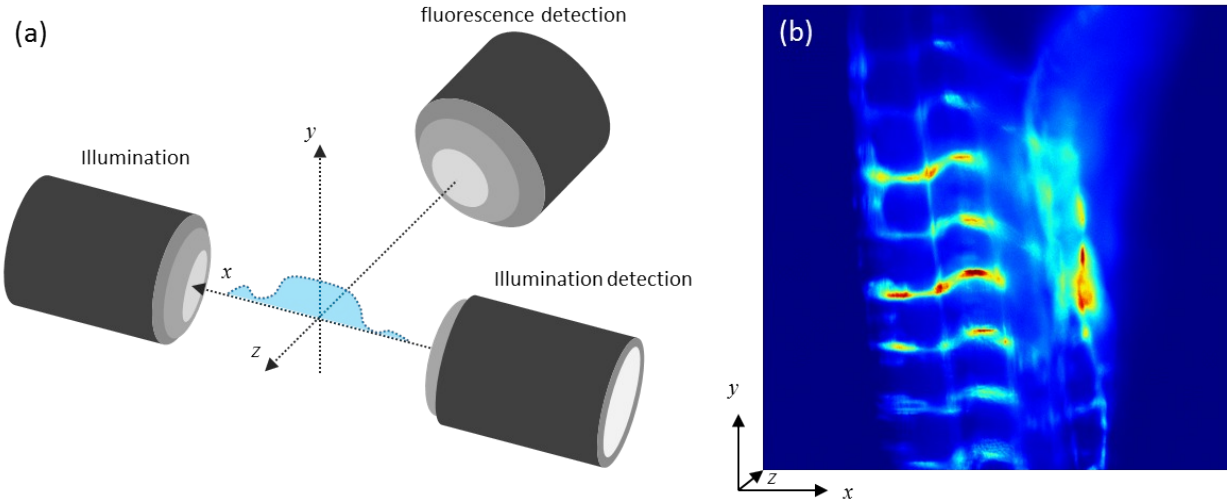

Figure 1. (a) A diagram showing the configuration of lenses in our adaptive LSFM setup. The fluorescence is detected orthogonally to the illumination. (b) A standard LSFM image of a fixed Fli:EGFP zebrafish tail with coordinate axes matching (a).

As a result of this LSFM tends to be used on larger specimens where the desire to image with the highest possible resolutions is not required, but to image fast, in 3D and with reasonable quality. In this case, however, the increase in the size of the samples increases the inhomogeneity of the optical path, the scattering and the absorption and thus degrades the performance of microscope significantly. For this reason many of the larger samples are chemically treated[7] or genetically modified[8] before imaging to increase their transparency and optical quality.

In conclusion, for both larger and smaller samples it is clear that adaptive optics (AO), namely the ability to control the phase of the illumination light and the detection light, could significantly improve this technology. In this paper the use of adaptive optics in the illumination path of a LS microscope is presented alongside the use of wavefront shaping techniques to improve the LS profile.

2. APPROACHING ADAPTIVE OPTICS IN LSFM

Adaptive optics has the goal of improving the quality of the images that the microscope produces. These adaptive systems require three parts: a wavefront sensor, a wavefront reconstructor and a wavefront corrector.

There are broadly speaking two approaches to wavefront sensing,[9] one uses a pupil plane sensor and the other known as *sensorless* uses a focal plane sensor. In pupil-plane sensors the gradient or the curvature of the wavefront in the pupil is measured. This information is then used by the wavefront reconstructor to calculate the phase profile in the pupil. Afterwards the inverse of this phase is applied to the corrector so that the wavefront is flattened, therefore, giving a corrected image. For a focal-plane sensor, instead the information from the recorded image is extracted into a mathematical form that can be optimized through a algorithm to ultimately yield better image.

LSFM uses wide-field (WF) imaging and therefore, the problem is made harder by the fact that we are imaging extended objects and not collecting light from a single point as with confocal techniques. Wavefronts are defined as the surface of constant phase for a point-source, not extended sources. Therefore, pupil plane detectors are not designed to work with extended sources. It is possible to include fluorescent microspheres in the sample to act as artificial point sources[10] so that you can perform direct sensing; however, it is not very practical for biological imaging in live tissues. The problems arise when alien material is introduced as it can cause a response from the organism. This is to be avoided if one wants to faithfully approximate the natural state of the organism in the microscope. Furthermore, when looking at point-like objects what is "perfect" is known, namely a diffraction-limited Airy disc. In wide-field imaging, the true "perfect" image is not known.

Since there is no way to determine whether you have the best solution, the design of the image quality metric to give meaningful improvements in contrast is of utmost importance.

In LSFM we want to solve the following problem, where σ is the metric that defines the quality of the images produced, for example, it could be a measure of the high spatial frequency content of the image:

$$\max_{\phi,\varphi} \sigma(\phi, \varphi) \tag{1}$$

Here the phase in the pupil plane of the illumination objective, ϕ, and the fluorescence pupil plane phase, φ, are our decision variables. What pupil plane phase will produce the maximum image quality. The solution are the values of ϕ and φ to apply in these pupils such that the image quality is maximized. Since it would take an impractically long time to try all the various combinations allowed by the adaptive elements, this problem is solved by optimization techniques.

There are two broad approaches to the optimization, one is based on taking measurements on the experimental system whilst making perturbations until the algorithm converges, known as *model-free*; and the second makes a model of the system and performs the optimization on the model, known as *model-based*. Unfortunately, the peculiarities of optical systems make it the worst possible kind of optimization problem to solve. Equation 1 shows a non-convex and non-linear function and to further complicate matters the measurements in general are noisy. This means that the problem as it is written above would not yield any meaningful results in the vast majority of cases. Nevertheless, approaches to sensorless adaptive optics, both model-free and model-based have yielded promising results in microscopy.[11–13]

AO has been successfully included into the LSFM[14,15] with the focus on the correction of aberrations in the imaging arm. These approaches are a mixture of model-free and model-based approaches to correcting the aberrations. In this paper we will focus on the optimization of the illumination for use in the LSFM.

3. THE ADAPTIVE LSFM SYSTEM

In the standard configuration of a LS microscope the only signal acquired is images of the fluorescence signal. From this data it is possible to compute an image quality metric σ, however, very little information is given about the thickness, length, or uniformity of the LS. This information is mostly lost as the light arriving at the camera comes only from areas containing fluorophores; therefore, placing another imaging camera into the setup to capture the transmitted laser light would allow access to this information.

To control this illumination light it is desired to have many degrees of freedom as possible to correct higher order aberrations. Since the laser light is a polarized coherent source a spatial light modulator (SLM) is best used for this purpose. On the detection side, it is desired to be able to control the focal plane of the microscope and remove aberrations. The light source in this case is incoherent fluorescence, therefore, a high stroke, small aperture deformable mirror is desired.

We have realized such as a system using a liquid-crystal phase only SLM (512x512, Boulder/Meadowlark, US) in the illumination path and a 69-actuator deformable mirror (DM) (DM69, Alpao, France). These two components allow full adaptive and wavefront control over the light in the LS microscope. In Figure 2 the schematic of the experimental setup is shown. At the centre there is a custom designed and 3D printed acrylic (Shapeways, Netherlands) sample chamber with three ports for objective lenses (2x UMPLFLN 10x, 1x UMPLFLN 20x Olympus, Japan) sealed so that the chamber is water tight. The samples are mounted in agarose gels and suspended by glass capillaries above the samples. A 4D translation shape is used (USB 4D Stage, Picard Industries, U.S.) for coarse sample movement and alignment. Fine adjustments of the illumination focus and LS position are done optically using tip-tilt and defocus actuation on the SLM with corresponding focal compensation on the DM. This ensures that the plane of the LS is coplanar with the detection objective focal plane.

The fluorescence light is captured through the 20x objective is relayed onto the DM and captured on an sCMOS camera (Orca Flash 4, Hamamatsu Photonics, Japan). The transmission light is imaged through a 10x objective and a tube lens (AC254-300-A-ML, Thorlabs, U.S.) onto a CMOS camera (DCC1545M, Thorlabs, US).

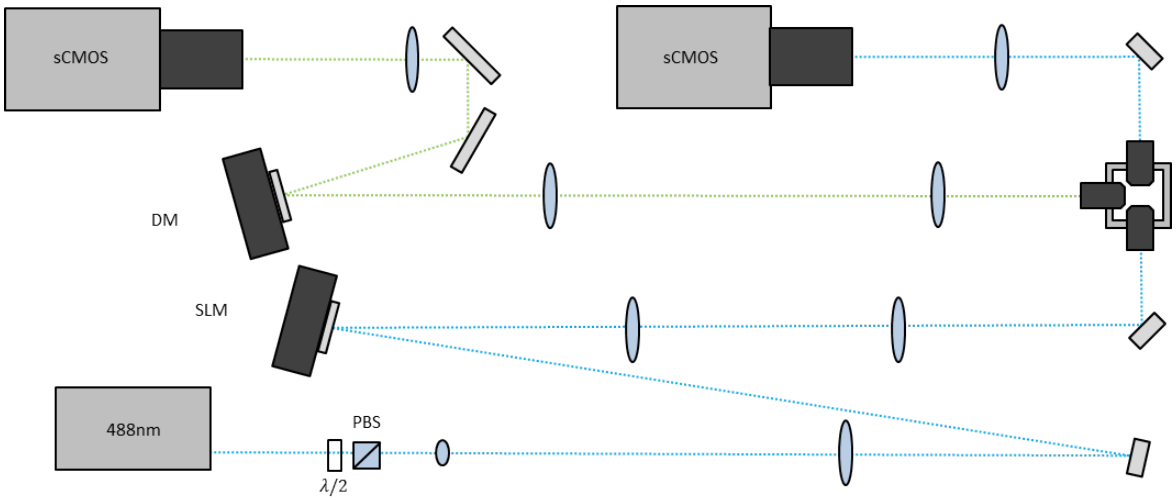

Figure 2. A schematic showing the realization of the system setup for full adaptive control of the LS microscope. A 488nm laser source is used to illuminate the SLM after polarisation control and expansion. The image of the SLM is conjugated with the back aperture of the illumination objective after zero order correction. The fluorescence light is collected and imaged on a sCMOS camera via the DM for focus and correction. The transmitted light is collected and used to feedback and control the illumination.

In addition, using the transmitted light on the camera the beam shape and quality can be adapted. Both the light captured by both the cameras is used for the optimization of the image quality.

The SLM is not conjugated to the back aperture of the illumination objective as would be conventional. In order to remove the effect of the zeroth order reflection from the SLM surface, a corrective procedure must be implemented. The corrector consists of a permanent defocus applied to the SLM and a beam blocking pinhead. The zeroth order light does not undergo the SLM phase change and it is focused by the first lens (AC508-180-A-ML, Thorlabs, U.S.) onto a pinhead. The defocused higher orders are not blocked and come into focus around 50mm after the pinhead. They are sufficiently defocused such that the performance of the SLM is not noticeably affected by this procedure. At this first order focus a slit is placed to block the second order light and to prevent the formation of the three LSs in the sample chamber. A second lens (AC508-200-A-ML, Thorlabs, U.S.) relays the image of the SLM, minus the defocus, onto the back aperture of the illumination objective.

4. LIGHT-SHEET CORRECTION AND SHAPING

4.1 Light-sheet Correction

Before the shape of the LS is optimized, the beam aberrations are minimized by the maximization of the variance of an region-of-interest (ROI) over the LS on the transmission camera. For the diffraction-limited Gaussian beam this method is adequate, however, for a more complex beam structure this will not converge to the optimum solution. The optimization is performed using a custom algorithm[16] that is robust to the measurement noise and uses M Zernike modes as a basis for the SLM phase. With N pixels in the ROI, the optimization is mathematically described as:

$$\max_{\alpha} \frac{1}{N} \sum_{n=1}^{N} \left(i_n(\alpha) - \frac{1}{N} \sum_{n=1}^{N} i_n(\alpha) \right)^2 \tag{2}$$

Here i_n refers to the n-th pixel value in the ROI, it is a function of α the coefficients of the Zernike series expansion $\phi = \sum_{m=1}^{M} \alpha_n \mathcal{Z}_n$. For a simple test of this method we place a sample of fluorescence beads embedded in 2% agarose gel inside a glass capillary in the microscope. Figure 3 shows the improvement in the beam profile at the focal position of the LS before and after correction using this technique. In this case the sample is 2% agarose gel in a glass capillary tube. $M = 5$ Zernike modes were used in correction on an ROI 64x64px and 100 iterations of the algorithm were run to ensure convergence.

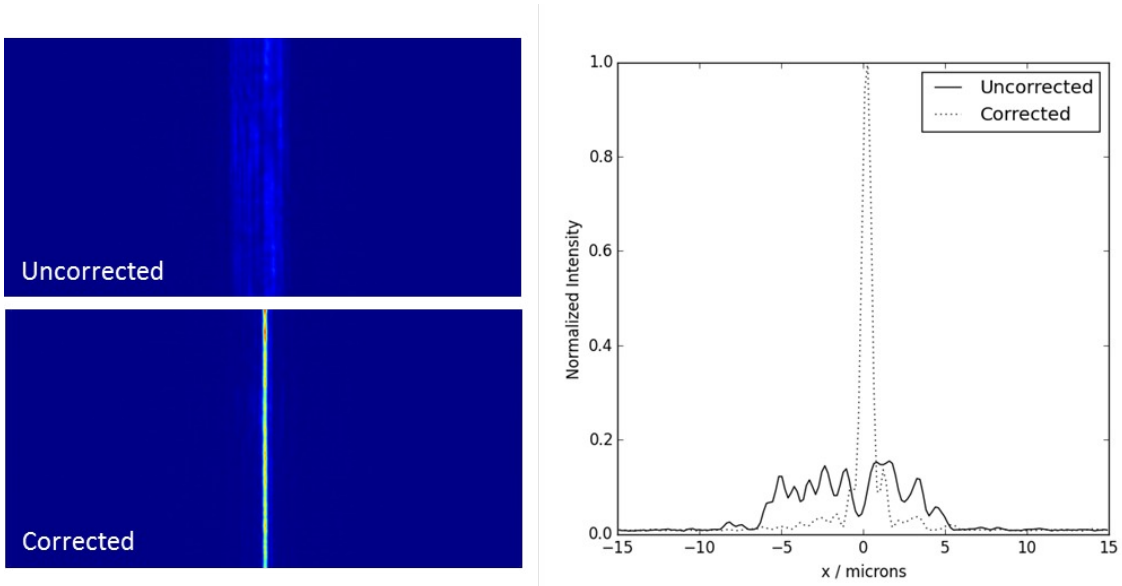

Figure 3. Representations of the beam profiles of the LS at the focus before and after correction. On the left are the images from the transmission camera and on the left the line profile through the center of the field-of-view. The sample, through which the LS passes, is fluorescence beads embedded in 2% agarose gel inside a glass capillary tube.

4.2 Light-sheet Shaping

After this correction is applied the LS is then shaped. As stated previously the profile of the standard Gaussian beam does not produce the optimum LS for imaging. The ideal LS for imaging would be as thin as possible and would be uniform in intensity and thickness over a long range. These are not the properties of the Gaussian beam which diverges from the focus decreasing the on axis intensity and increasing the out-of-focus light.

There have been already many approaches to this problem in the literature such as Bessel beams,[17] Airy beams[18] and aspheric systems.[19] Here we take a different approach and form a metric for the quality of the LS. Since the SLM allows us to shape the profile of the focal intensity by modifying the phase in the illumination pupil, we use wavefront shaping[20] to find our optimal LS. This mathematical problem is hugely under-determined due to phase diversity, that is there are many possible phase patterns that give the same intensity at the focal position. Therefore, to find the best phase profile on the SLM we have designed a metric that is suitable for the purpose of evaluating the quality of the LS. Images I_k are taken on the transmission camera at K positions over a range of Δ.

$$\text{r.m.s.} = \rho = \sqrt{\frac{1}{K}\sum_{k=0}^{K}(I_k - \max(I_k))^2} \tag{3}$$

The r.m.s. is essentially the deviation from the ideal LS. A LS that is flat along the optical axis has a value of zero. The range of Δ effects the number of positions are needed for the optimization to converge to the global minimum. A larger value of Δ requires more positions than a smaller value, this is due to the size of the PSF. The longer the range the blinder the metric becomes to non-ideal optimizers of the problem for the same number of measurements, i.e. there are more local minima for the algorithm to converge to.

Visually, with $K = 3$ it is possible to have a long flat axial section, or it is possible to have three humps. All of these will technically give the same value for the objective, but they will not be the solutions that we want to find. Moreover, it is necessary to be very particular with the functions that one chooses to apply to the SLM in order to extend the depth of field. Whilst a common approach is to use cubic or axicon functions, this is not ideal for LSFM since the PSF becomes distorted and asymmetric. Furthermore, complex pupil functions in the general case tend to produce asymmetric axial PSFs.

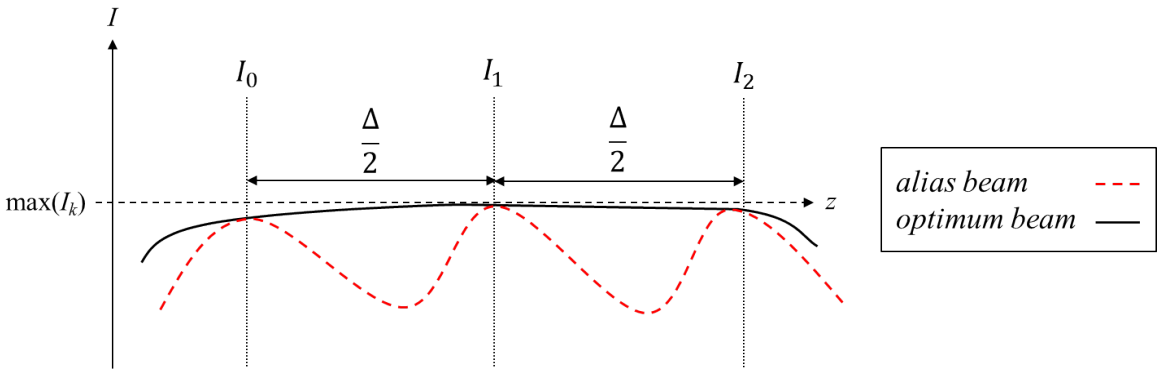

Figure 4. A visualization of the metric used to shape the beam profile. If an insufficient number of measurements is taken aliasing can occur in finding the solution.

Our approach uses binary pupil filters (PF)[21] to provide an extended depth of field to the focused LS. Unlike the other most other commonly used beam forming techniques, that is the Gauss-Bessel beam or the Gaussian beam it has a uniform axial profile along the sheet for a given range. The pupil function is real valued ± 1 and therefore, the solution is symmetric along the optical axis and in the orthogonal directions. These pupil filters are found by a two-stage optimization procedure[22] of the step changes and are effective at keeping the axial resolution over the central range uniform. Essentially, the positions of the step changes m_i's for M positions are optimized, where $\mathbf{m} \in \mathbb{R}^M$,

$$\begin{aligned} &\min_{\mathbf{m}} \ \rho(\mathbf{m}, \Delta) \\ &\text{s.t. } m_i + \delta < m_{i+1} \end{aligned} \tag{4}$$

Here δ is included as a constraint. This is the width of a Fresnel zone in the pupil, essentially, if elements are closer than a Fresnel zone they will exhibit no influence on the shape of the focused beam. For this reason, it is only possible to find solutions to the PF up to and including the number of Fresnel zones in the pupil. The profile along the direction of the light-sheet propagation is shown in Figure 5. Here the intensity is normalized so that they both have the same intensity at the focal position.

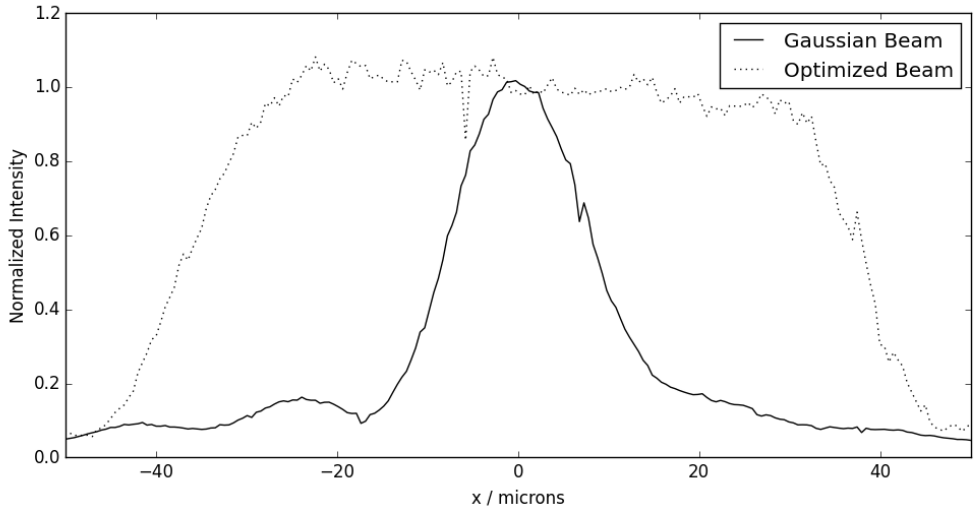

Figure 5. The x-axis profile of a LS as viewed from the fluorescence objective in the focal plane. The optimization of the pupil phase is able to extend the region over which the light-sheet is uniform.

The effect of the PF phase profile is to extend the region over which the beam is constant. In the example shown in Figure 5 a 4.2× full-width at half-maximum (FWHM) axial extension for a 1.6× increase in lateral beam size is seen. For comparison decreasing the NA by 1.6× would only yield an increase of 2.6× and it would not produce this flat intensity across the focal range. Equally, the PFs have the advantage that they are designed for the specific pupil and they are a phase only technique meaning no laser power is lost.

5. DISCUSSION

In this paper we have outlined how the use of adaptive optics to control the illumination in a LS microscope may be implemented. We have discussed our experimental setup and our approaches to the shaping of LS for LSFM and correction of aberrations in the illumination path.

The challenges that remain are to integrate the shaping and the aberration correction within thick, scattering and complex samples. We have found that with no correction applied, the aberrations introduced by these samples mean that whatever wavefront shaping is applied to the LS, it will be scrambled by the sample and appear in fluorescence signal no different to that of a Gaussian beam. Hence, it is imperative to increase the number of spatial frequencies that can be corrected. Once applied this will bring better optical sectioning to the LSFM in thick samples regardless of the beam shape used.

Furthermore, it is not simply enough in the LS microscope to correct for the illumination alone. The light that is emitted from the sample has to pass through a large amount of refracting tissue before it reaches the detection camera. Whilst we have used model-free optimization in the calibration of the deformable mirror with fluorescence microspheres, it has not yet been successfully applied to thick samples.

The system we have presented along with the preliminary data shows that with the correct development of algorithms and models, this system would be able to correct for the scattering, aberrations and perhaps some of the absorption that causes LSFM images to be degraded.

ACKNOWLEDGMENTS

This work is sponsored by the European Research Council, Advanced Grant Agreement No. 339681. The authors would like to thank the contributions of W.J.M. van Geest and C.J. Slinkman.

REFERENCES

[1] Voie, A., Burns, D., and Spelman, F., "Orthogonal-plane fluorescence optical sectioning: Three-dimensional imaging of macroscopic biological specimens," *Journal of microscopy* **170**(3), 229–236 (1993).

[2] Huisken, J., Swoger, J., Del Bene, F., Wittbrodt, J., and Stelzer, E. H., "Optical sectioning deep inside live embryos by selective plane illumination microscopy," *Science* **305**(5686), 1007–1009 (2004).

[3] Santi, P. A., "Light sheet fluorescence microscopy a review," *Journal of Histochemistry & Cytochemistry* **59**(2), 129–138 (2011).

[4] Tokunaga, M., Imamoto, N., and Sakata-Sogawa, K., "Highly inclined thin illumination enables clear single-molecule imaging in cells," *Nature methods* **5**(2), 159–161 (2008).

[5] Dunsby, C., "Optically sectioned imaging by oblique plane microscopy," *Optics express* **16**(25), 20306–20316 (2008).

[6] Born, M. and Wolf, E., [*Principles of Optics*], Cambridge University Press.

[7] Dodt, H.-U., Leischner, U., Schierloh, A., Jährling, N., Mauch, C. P., Deininger, K., Deussing, J. M., Eder, M., Zieglgänsberger, W., and Becker, K., "Ultramicroscopy: three-dimensional visualization of neuronal networks in the whole mouse brain," *Nature methods* **4**(4), 331–336 (2007).

[8] White, R. M., Sessa, A., Burke, C., Bowman, T., LeBlanc, J., Ceol, C., Bourque, C., Dovey, M., Goessling, W., Burns, C. E., et al., "Transparent adult zebrafish as a tool for in vivo transplantation analysis," *Cell stem cell* **2**(2), 183–189 (2008).

[9] Booth, M. J., "Adaptive optics in microscopy," *Philosophical Transactions of the Royal Society A: Mathematical, Physical and Engineering Sciences* **365**(1861), 2829–2843 (2007).

[10] Azucena, O., Crest, J., Kotadia, S., Sullivan, W., Tao, X., Reinig, M., Gavel, D., Olivier, S., and Kubby, J., "Adaptive optics wide-field microscopy using direct wavefront sensing," *Optics letters* **36**(6), 825–827 (2011).

[11] Débarre, D., Botcherby, E. J., Watanabe, T., Srinivas, S., Booth, M. J., and Wilson, T., "Image-based adaptive optics for two-photon microscopy," *Optics letters* **34**(16), 2495–2497 (2009).

[12] Booth, M. J., "Wavefront sensorless adaptive optics for large aberrations," *Optics letters* **32**(1), 5–7 (2007).

[13] Antonello, J., van Werkhoven, T., Verhaegen, M., Truong, H. H., Keller, C. U., and Gerritsen, H. C., "Optimization-based wavefront sensorless adaptive optics for multiphoton microscopy," *JOSA A* **31**(6), 1337–1347 (2014).

[14] Bourgenot, C., Saunter, C. D., Taylor, J. M., Girkin, J. M., and Love, G. D., "3d adaptive optics in a light sheet microscope," *Optics express* **20**(12), 13252–13261 (2012).

[15] Masson, A., Escande, P., Frongia, C., Clouvel, G., Ducommun, B., and Lorenzo, C., "High-resolution in-depth imaging of optically cleared thick samples using an adaptive spim," *Scientific reports* **5** (2015).

[16] Verstraete, H. R. G. W., Wahls, S., Kalkman, J., and Verhaegen, M., "Model-based sensor-less wavefront aberration correction in optical coherence tomography," *Optics Letters* (2015).

[17] Planchon, T. A., Gao, L., Milkie, D. E., Davidson, M. W., Galbraith, J. A., Galbraith, C. G., and Betzig, E., "Rapid three-dimensional isotropic imaging of living cells using bessel beam plane illumination," *Nature methods* **8**(5), 417–423 (2011).

[18] Vettenburg, T., Dalgarno, H. I., Nylk, J., Coll-Lladó, C., Ferrier, D. E., Čižmár, T., Gunn-Moore, F. J., and Dholakia, K., "Light-sheet microscopy using an airy beam," *Nature methods* **11**(5), 541–544 (2014).

[19] Saghafi, S., Becker, K., Hahn, C., and Dodt, H.-U., "3d-ultramicroscopy utilizing aspheric optics," *Journal of biophotonics* **7**(1-2), 117–125 (2014).

[20] de Visser, C. C. and Verhaegen, M., "Wavefront reconstruction in adaptive optics systems using nonlinear multivariate splines," *JOSA A* **30**(1), 82–95 (2013).

[21] Sheppard, C. J., "Pupil filters for generation of light sheets," *Optics express* **21**(5), 6339–6345 (2013).

[22] Wilding, D., Pozzi, P., Soloviev, O., G, V., Sheppard, C. J., and Verhaegen, M., "Pupil filters for extending the field-of-view in light-sheet microscopy," *Optics Letters* (2016, in review).